Instabilities of the Stewartson Layer II. An Experimental/Numerical Comparison

Tamar More[1], Birgit Futterer, Rainer Hollerbach[2], Christoph Egbers

Dept of Aerodynamics and Fluid Mechanics, Brandenburg Tech. Univ., 03013 Cottbus, Germany

ABSTRACT

In the preceding contribution in this volume (Hollerbach [1]), we introduced the general Stewartson layer problem, and considered the linear onset of non-axisymmetric instabilities, which we found to be very different for positive versus negative differential rotation of the inner sphere. In this work we focus primarily on the positive differential rotation case, but now consider the nonlinear, fully three-dimensional equilibration of these instabilities, and find that in the increasingly supercritical regime a series of mode transitions occurs in which the azimuthal wavenumber is successively reduced by one each time. We also present experimental results in good agreement with the numerical results.

The experimental setup is that of Egbers & Rath [2]. It consists of concentric spheres of radii $r_i = 26.70$ mm and $r_o = 40.00$ mm, which can be independently rotated about a common axis at speeds up to 850 rev/min. The fluid filling the gap is M3 silicone oil, having a viscosity of $\sim$ 3 cSt. In terms of the Ekman number $E = \nu/\Omega_o(r_o - r_i)^2$ introduced in [1], we can therefore reach values as small as $10^{-3.1}$. Although this is not nearly as small as the 10^{-5} considered in [1], it turned out to be small enough, as this progression to higher and higher wavenumbers noted in [1] very conveniently seems to occur much quicker in the thinner gap considered here (with $r_i/r_o = 2/3$ rather than $1/3$ as in [1]).

We begin by presenting the numerical results. Then, once we have a clearer idea of what we are looking for, we will return to the experimental results, where our visualization technique (aluminium flakes mixed in with the fluid) allowed us to detect the azimuthal mode number of the instability, and which we find to be in good agreement with the numerical results.

As in Fig. 1 of [1], Fig. 1 here also shows contours of the angular velocity, for Ekman numbers from $10^{-2.5}$ to $10^{-3.1}$. We again see the emergence of the Stewartson layer on the tangent cylinder. Because the inner sphere is now much bigger than before, the layer is correspondingly crowded into the equatorial region. Nevertheless, we see that this range of Ekman numbers is already small enough for a well-defined shear layer to exist. Figure 2 then shows the linear onset of instability, although this time only for $Ro > 0$. We see the same progression to higher and higher m as in [1], only much quicker, with a factor of 4 in E being sufficient to progress from 3 to 6.

Everything thus far is much as in [1], just at a different gap width. We now proceed beyond [1] though, and consider the nonlinear equilibration in the supercritical regime. Suppose we fix E at $10^{-3.1}$, for example, and gradually increase Ro. According to Fig. 2, the most unstable mode is then $m = 6$, with $Ro_c = 0.237$. In the slightly supercritical regime, we would therefore expect the instability to equilibrate at some finite amplitude, and to contain only multiples of this basic wavenumber $m_0 = 6$. This is exactly what was observed up to $Ro = 0.306$. Beyond that value, however, this $m_0 = 6$ solution is unstable, and the system instead switches to an $m_0 = 5$ solution. Increasing Ro further, at 0.432 this in turn yields to $m_0 = 4$, and so on down to $m_0 = 3$. And if one then decreases Ro again, one obtains the whole sequence in reverse, although with a considerable degree of hysteresis. Figure 2 also shows the critical Rossby numbers for these supercritical mode transitions.

[1]Permanent Address: Department of Physics and Chemistry, University of Portland, Portland OR 97203, USA

[2]Permanent Address: Department of Mathematics, University of Glasgow, Glasgow, G12 8QW, United Kingdom

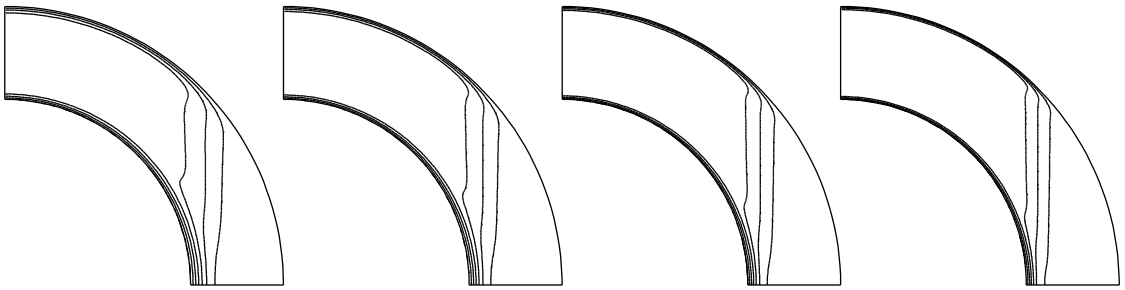

Figure 1: Contours of the angular velocity, for $Ro = 0$ and, from left to right, $E = 10^{-2.5}$, $10^{-2.7}$, $10^{-2.9}$ and $10^{-3.1}$. The contour interval is 1/7.

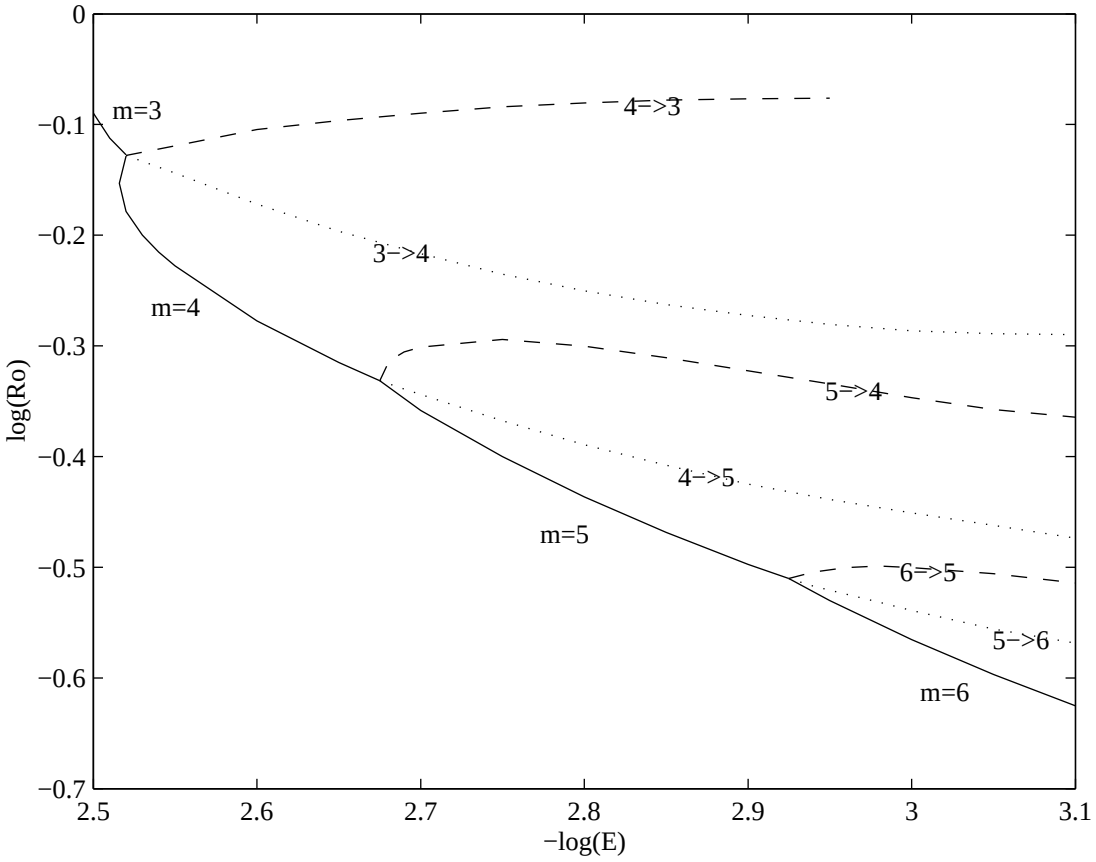

Figure 2: The solid lines labelled '$m = \ldots$' are the linear onset curves of the indicated modes. The dashed lines labelled '$m -> m - 1$' are the transitions obtained when increasing Ro, and finally the dotted lines labelled '$m -> m + 1$' are the reverse transitions obtained when decreasing Ro again.

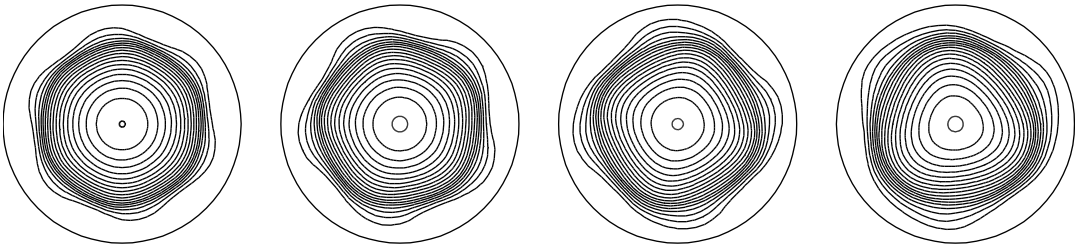

Figure 3: From left to right, the solutions at $Ro = 0.3$, 0.4, 0.5 and 0.6, and all four at $E = 10^{-3.1}$.

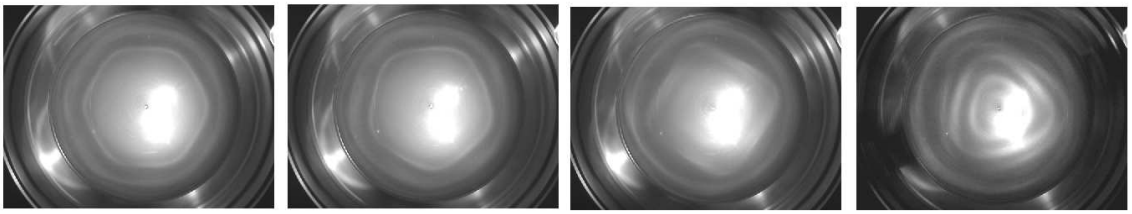

Figure 4: Photographs of the experiment, showing $m_0 = 6$, 5, 4 and 3 modes, just as in Fig. 3.

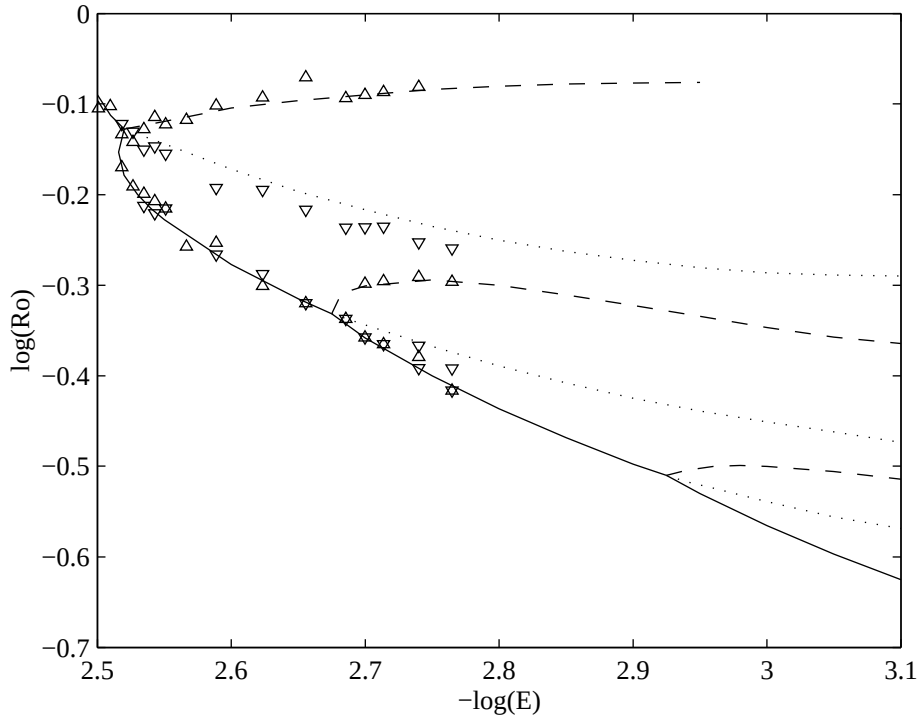

Figure 5: As in Fig. 2, but now also showing the experimental results. Upward/downward pointing triangles denote transitions obtaining by increasing/decreasing Ro. (The experimental results beyond $E = 10^{-2.75}$ have not been measured yet, but this is still planned, and these additional results will hopefully agree equally well.)

Finally, Fig. 3 shows what the solutions actually look like. What is shown is the streamfunction of the vertically integrated horizontal flow. That is, if $\mathbf{U} = (U_z, U_s, U_\phi)$, consider

$$\mathbf{V}_H = \left(0, \int U_s \, dz, \int U_\phi \, dz\right).$$

By construction this flow is independent of z, so it has a streamfunction representation. Also, since the original $\mathbf{U}$ is almost independent of z (the pattern seen in Fig. 1 persists into the nonlinear, fully 3D regime), $\mathbf{V}_H$ will indeed be the dominant part of the flow. Showing its streamfunction is therefore the most compact way of representing the essential features of the solution. So, we see then in Fig. 3 how the originally circular Stewartson layer is distorted first into a hexagon, then a pentagon, a square, and finally a triangle, corresponding to this progression from $m_0 = 6$ to 3. Further details of the numerical solutions will also be presented in the poster.

Returning finally to the experiment, these results largely describe themselves. Figure 4 shows photographs looking straight down onto the apparatus. We note first of all that while the visualization is incapable of revealing fine details of the Stewartson layer, it is more than adequate for determining the azimuthal wavenumber m. And better still, comparing Figs. 3 and 4, we see that the agreement is quite good. Next, Fig. 5 shows how the experimentally determined mode transitions agree with the numerically computed ones, with the agreement again rather good. And again, further details of the experimental results will be presented in the poster.

REFERENCES

[1] R. Hollerbach *Instabilities of the Stewartson layer,* Abstract in this volume.

[2] C. Egbers, H.J. Rath *The existence of Taylor vortices and wide-gap instabilities in spherical Couette flow,* Acta Mech. **111**, 125–140, 1995.